Int J Clin Exp Med 2019;12(3):2374-2383
www.ijcem.com /ISSN:1940-5901/IJCEM0087796

Original Article

MiRNA-466c modulates blood-brain barrier permeability upon cerebral ischemia via targeting IGF-1

Zhijun Ye, Xiang Bao, Gezhi Zhou, Fengfeng Jiang, Wei Xu

Department of Neurosurgery, Jinhua Central Hospital, Jinhua, 321001, Zhejiang Province, China

Received November 2, 2018; Accepted December 10, 2018; Epub March 15, 2019; Published March 30, 2019

Abstract: Background: Blood-brain barrier (BBB) permeability has essential roles in brain injury upon cerebral ischemia. MicroRNAs (miRNAs) are used as potential therapeutics involved for multiple types of brain damage. A broader view of which miR-466c interacts with BBB permeability upon cerebral ischemia is required. Methods: Middle cerebral artery occlusion (MCAO) surgery in Sprague Dawley rats and oxygen-glucose deprivation (OGD) in Sprague Dawley rat primary brain microvascular endothelial cells (BMECs) were subjected to cerebral ischemia model establishment. Quantitative reverse transcription PCR (qRT-PCR) assays were used to examine the abundance of miR-466c and insulin-like growth factor-1 (IGF-1) either in Sprague Dawley rats or BMECs. Luciferase assay was performed to probe the interactions between miR-466c and IGF-1. Cresyl violet stain, Evans blue and FITC-dextran leakage assay were conducted to investigate the effect of miR-466c and IGF-1 on BBB permeability induced by cerebral ischemia. Results: Cerebral ischemia induced a strong reduction of miR-466c and a great increase of IGF-1 abundance. Accumulation of miR-466c increased neurological score, brain water content, infarct volume, and BBB permeability. Concordantly, IGF-1, as a direct target, was limited by miR-466c in BMECs. In addition, IGF-1 protected BBB permeability in the presence of abundant miR-466c upon cerebral ischemia. Conclusions: miR-466c has a vital role in BBB permeability via targeting IGF-1 *in vivo* and *in vitro*, providing a promising therapeutic for cerebral ischemia.

Keywords: Blood-brain barrier, cerebral ischemia, miR-466c, IGF-1, MCAO, OGD

Introduction

Cerebral ischemia is a key driver of brain damage afflicting a mounting number of people worldwide via sudden death or cognitive dysfunctions [1]. Disruption of the blood-brain barrier (BBB), interposed between the circulatory system and the central nervous system, is a major pathological feature in terms of brain damage and interacts with multiple factors at different stages of cerebral ischemia [2]. Hence, protection of BBB integrity upon cerebral ischemia is a promising therapeutic approach and warrants more attention.

Notably, microRNAs (miRNAs) might be required for BBB dysfunction involved in neurological disorders through modulating gene abundance [3, 4]. To date, miR-210 disrupted BBB integrity by blocking junction proteins during ischemic brain injury [5]. Apart from miR-210, miR-337 is also essential for cerebral ischemia and coordinates with brain injury and neurological deficits [6]. Furthermore, a recent review described miRNA-based therapeutics that were functionally related to BBB protection during central nervous system injuries [7]. There have been few efforts in support of the miR-466 family being shown in brain damage except reduction abundances of miR-466a and miR-466d in neural stem cells on hyperglycemia [8].

miRNAs contribute to brain insult via modulating mRNA expression on ischemic [9]. Generally, insulin-like growth factor-1 (IGF-1) is essential for cerebral protection and ischemic stroke [10, 11]. Faced with ischemic brain damage, reduction of IGF-1 contributed to BBB leakage in C57BL/6 mice [12]. In contrast, sodium butyrate treatment increased the abundance of IGF-1 and reduced BBB permeability in Sprague Dawley rats after middle cerebral artery occlusion (MCAO) [13]. The available evidence indicates that IGF-1 is a neuro-protectant and pro-

vides a possible therapeutic target upon brain injury [14, 15]. Since IGF-1 opens up the possibility of BBB protection, mechanisms that underlie the interaction with miR-466c remain elusive. In the present study, regulation of miR-466c on BBB permeability upon cerebral ischemia was investigated via perfecting the models of MCAO *in vivo* and oxygen-glucose deprivation (OGD) *in vitro*.

Methods

Animals and model of MCAO

Adult male Sprague Dawley rats, weighing 250-300 g, were obtained from the China National Laboratory Animal Resource Center (Shanghai, China). All rats were acclimatized to maintenance in specific pathogen-free, humidity and temperature-controlled microisolator cages with a 12 hour light/dark cycle for one week. Water and food were free access during the experiments. Every effort was made to minimize animals (n=7/group) during the study and studies were performed in accordance with the Guiding Principles in the Use of Laboratory Animals and approved by the Committee of Jinhua Central Hospital.

For the model of transient cerebral ischemia, rats were anesthetized with 10% chloral hydrate (Sigma, Saint Louis, MO, USA) and then subjected to MCAO surgery as described previously [16]. Briefly, a midline incision was made to isolate the right common carotid artery, external carotid artery, and internal carotid artery. Then a silicon-coated nylon 4.0 suture (Doccol Corporation, Redlands, CA, USA) was introduced into the internal carotid artery to occlude the origin of the middle cerebral artery. After 90 minutes of MCAO surgery, the suture was withdrawn. The sham surgery group experienced the similar insult without suture insertion. During the surgery, rectal temperature was maintained at 37±0.5°C using a homeothermic heating pad.

To explore the function of miR-466c, miR-466c mimics or control (Thermo Fisher, Wilmington, DE, USA) was given via the right lateral ventricle through a stereotactic apparatus within 30 minutes after MCAO. The rats were euthanized at the time points 6, 24, or 72 hours following MCAO. Brain tissue samples in ischemic core and contralateral hemisphere were collected and stored at -80°C until required.

Brain water content

Suffering from the introduction of miR-466c for 24 hours, brains were collected and immediately weighed. Then the brains were dried for approximately 24 hours at 110°C and weighed again. The brain water content was calculated as (wet weight-dry weight)/wet weight × 100%.

Evans blue leakage assay

After the injection of miR-466c mimics, 2% Evans blue dye (Sigma) was administered to animals via right femoral vein. After 2 hours, the rats were perfused with phosphate buffer saline (PBS, Sigma) through the left ventricle to remove the intravascular dye. The brain were excised, weighed, and incubated with formamide (Sigma) at 37°C for 24 hours before centrifugation at 2,000 × g for 20 minutes. The density of supernatant was measured at 632 nm using spectrophotometrically (Analytik Jena, Jena, Germany), and the content of Evans blue was calculated based on the stand curve. Extravasation of Evans blue was quantified as μg/g brain tissue.

Neurological evaluation and cresyl violet staining

Neurological deficit of rats was evaluated following the instructions of a five-tiered grading system at 24 hours after MCAO (0, no deficit; 1, failure to extend right paw; 2, spin longitudinally; 3, falling to the right; 4, unable to walk spontaneously) [17]. After the evaluation of neurobehavioral, brains were removed and sectioned at 20 μm thickness that were used for cresyl violet staining. Briefly, the sections were incubated with 1% cresyl violet acetate (Sigma) for 10 minutes, followed by dehydrated in 70%, 80%, 95%, 100% ethanol and xylene at room temperature. The infarct volume was calculated using Image J software (National Institutes of Health, Bethesda, MD, USA) from 4 slices and then expressed as the percentage of infarction in whole brain.

BMECs culture and OGD

Sprague-Dawley rat primary brain microvascular endothelial cells (BMECs) were isolated following the instructions previously described [18]. Cells were cultured in glucose-free Dulbecco's Modified Eagle Medium (DMEM) (Gibco,

Carlsbad, CA, USA) and immediately transferred to a humidified anaerobic chamber containing an atmosphere of 95% N_2, and 5% CO_2 for 30 minutes. When the OGD model was induced, the culture solution was replaced with normal medium and cultured at 37°C for 2, 4, or 6 hours. The control BMECs were incubated in standardized DMEM without deprived of oxygen and glucose.

BMECs permeability assay

BMECs with miR-466c mimics, si-IGF-1 or pcDNA-IGF-1 transfection were seed into Trans-well chamber (Costar, Coning, NY, USA) at the density of 1×10^4. After 24 hours, the medium was discarded and 0.01% FIFC-dextran (Sigma) in DMEM was added into the upper chamber, while culture medium without FITC-dextran was added to the lower chamber. The medium in the lower chamber was collected after 2 hours. The fluorescence intensity was determined by fluorescence microplate reader (PerkinElmer, Waltham, MA, USA) at an excitation wavelength of 488 nm and emission wavelength of 510 nm. Permeability coefficient for FIFC-dextran was calculated as $(I_r \times V)/(I_d \times S)$, where I_r or I_d is the fluorescence intensity of the receiver or donor chamber, V is the volume of lower chamber and S is the surface area of cell monolayer.

Plasmid constructs and cell transfection

IGF-1 cDNA was amplified and sub-cloned in the BamH I and Kpn I sites of pcDNA3.1 (Invitrogen, Carlsbad, CA, USA) to construct the pcDNA-IGF-1 vector. The specific primer of IGF-1 was synthesized by Invitrogen as follows: Forward: 5'-CGGGATCCCTGCTAACCAATTCATTTCCAGA-3' and Reverse: 5'-GGGGTACCTCACTTATCGTCGTCATCCTTGTAATCAGCCTTGGGCATGTCCGTGT-3'. MiRNA control, miR-466c mimics, miR-466c inhibitor, IGF-1 small interfering RNA (si-IGF-1) (Thermo Fisher) or the pcDNA-IGF-1 plasmid was transfected into BMECs using Lipofectamine 2000 (Invitrogen) referring to the manufacturer's protocol. Transfection efficiencies were analyzed by qRT-PCR after 24 hours.

RNA extraction and qRT-PCR

Total RNA from brain tissues or BMECs was extracted using Trizol reagent (Invitrogen) according to the manufacturer's instructions. RNA purity was detected by a NanoDrop Spectrophotometer (NanoDrop, Wilmington, DE, USA) and a ratio between 1.8 and 2.0 was considered acceptable. Template RNA was incubated with Reverse Transcription Kit (Invitrogen) following the manufacturer's instructions. Then cDNA was diluted and used for qRT-PCR with SYBR green (Applied Biosystems, Foster City, CA, USA) detection with the following amplification protocol: 95°C for 10 minutes, 40 cycles of 95°C for 15 seconds, and 60°C for 1 minute. Results were analyzed with $2^{-\Delta\Delta Ct}$ approach using β-actin or U6 as housekeeping gene for normalization of IGF-1 or miR-466c. Primers were designed from Invitrogen: IGF-1 (Forward, 5'-GCTGGTGGACGCTCTTCAGT-3'; Reverse, 5'-TTCAGCGGAGCACAGTACAT-3'), GAPDH (Forward, 5'-GACAACTTTGGCATCGTGGA-3'; Reverse, 5'-ATGCAGGGATGATGTTCTGG-3'), miR-466c (Forward, 5'-CACTAGTGGTTCCGTTTAGTAG-3'; Reverse, 5'-TTGTAGTCACTAGGGCACC-3'), U6 (Forward, 5'-GCTTCGGCAGCACATATACTAAAAT-3'; Reverse, 5'-CGCTTCACGAATTTGCGTGTCAT-3'). All assays were repeated in triplicate during the study.

Western blots (WB)

Total protein was isolated in cell lysis buffer with 1% protease inhibitor (Thermo Fisher) and quantified by BCA assay kit (Sigma). Then denatured proteins were separated by SDS-PAGE gel, transferred to polyvinylidene difluoride (PVDF) membranes (Millipore, Billerica, MA, USA), and blocked with blocking reagent (Thermo Fisher) for 1 hour at room temperature. Subsequently, the membranes were incubated with primary antibodies anti-rat IGF-1 or GAPDH (Abcam, Cambridge, UK) overnight at 4°C, followed by hatched with secondary antibodies (Abcam) for 2 hours at room temperature. The protein blots were visualized using enhanced chemiluminescence (ECL) chromogenic substrate (Thermo Fisher). GAPDH was used as a standard for band intensities.

Luciferase assays

Putative miR-466c targeting IGF-1 was predicted by the online software TargetScan. The 3' untranslated regions (3'-UTR) sequences of IGF-1 containing the putative binding sites of miR-466c were cloned into pGL3 luciferase reporter vector (Promega, Madison, WI, USA) to generate the wide-type plasmid (IGF-1 3'-UTR WT). Site-directed mutagenesis of miR-466c complementary bases was cloned into the pGL3-control vector to construct mutant-type plasmid (IGF-1 3'-UTR Mut). IGF-1 3'-UTR WT or

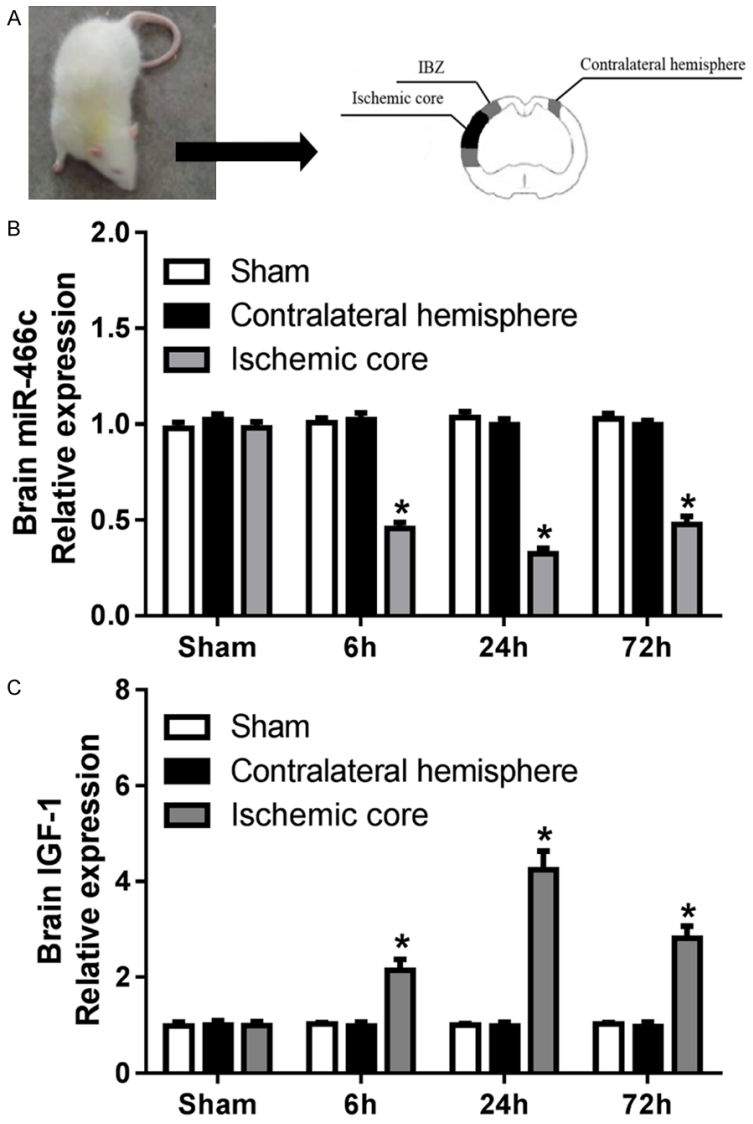

Figure 1. miR-466c expression is down-regulated and IGF-1 expression is up-regulated in ischemic core upon cerebral ischemia. (A) The sketches of ischemic core and contralateral hemisphere in brain tissue from MCAO rats and the abundance of miR-466c (B) and IGF-1 (C) were detected by qRT-PCR in ischemic core compared to sham group at 6, 24, and 72 hours after MCAO. n=7/group. *p< 0.05 versus sham group.

3'-UTR Mut plasmid was co-transfected with miR-466c mimics or miRNA control in BMECs using Lipofectamine 2000 according to the manufacturer's protocols. Transfected cells were lysed and contributed to the luciferase activities analysis by Luciferase Assay Kit (GeneCopoeia, Rockville, MD, USA).

Statistical analysis

Data are expressed as the mean ± standard deviation (SD) from three independent experiments. Statistical analysis was investigated by one-way analysis of variance (ANOVA) followed by Tukey's post hoc tests or Student's *t* test using GraphPad Prism 5 (GraphPad Inc., La Jolla, CA, USA). $p < 0.05$ was regarded as the level of statistically significant in all graphs.

Results

MiR-466c expression is impaired and IGF-1 expression is enhanced in ischemic core after MCAO

MCAO surgery was performed to determine the alterations in expression of miR-466c and IGF-1 in brain tissues upon cerebral ischemia. The sketches of ischemic core and contralateral hemisphere in brain tissue from MCAO rats are shown in **Figure 1A**. The abundances of miR-466c and IGF-1 in MCAO and sham groups were examined at 6, 24, and 72 hours after the surgery. The data revealed that MCAO induced a great loss of miR-466c abundance compared to sham group in ischemic core and described a trough of wave at 24 hours (**Figure 1B**). By contrast, abundance of IGF-1 was sharply enhanced with a peak at 24 hours in ischemic core suffering from cerebral ischemia (**Figure 1C**). As expected, little changes of miR-466c and IGF-1 levels were observed in contralateral hemisphere at different time points even though added same insult (**Figure 1B** and **1C**). Together, these findings suggested that both of miR-466c and IGF-1 had essential roles in response to cerebral ischemia.

Addition of miR-466c deteriorates cerebral ischemia-induced brain injury after MCAO

Given that miR-466c was aberrantly impaired on cerebral ischemia, the potential effect of miR-466c after MCAO *in vivo* was further inves-

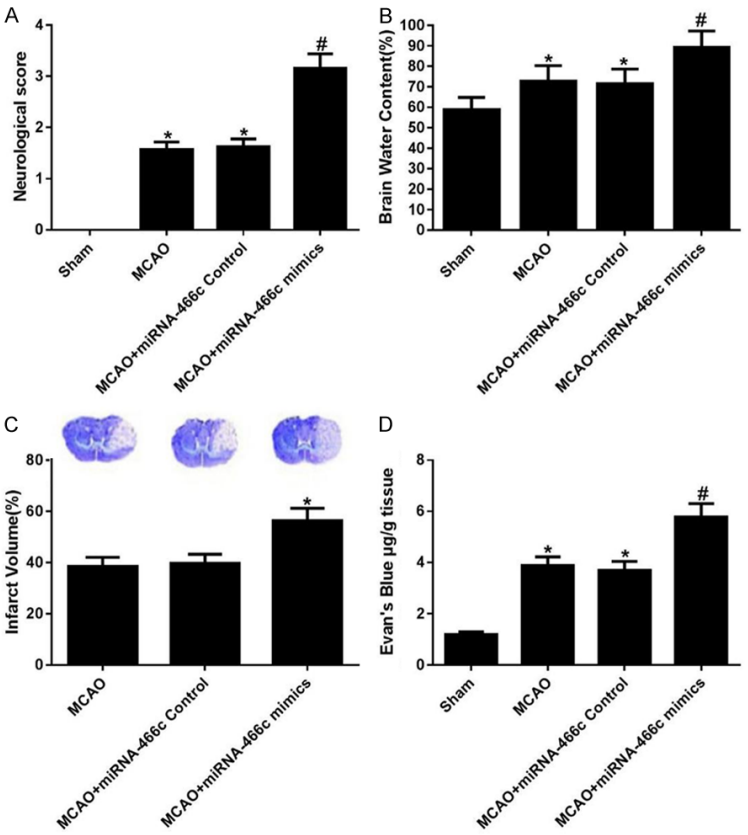

Figure 2. Addition of miR-466c exacerbates brain injury on cerebral ischemia after MCAO. A. Neurological deficit was investigated according the instructions of a five-tiered grading system in Sprague-Dawley rat after MCAO with miR-466c injection. *$p < 0.05$ versus sham group, #$p < 0.05$ versus MCAO + miR-466c control. B. The brain water content after MCAO was detected via wet-dry weight assay. *$p < 0.05$ versus sham group, #$p < 0.05$ versus MCAO + miR-466c control. C. Infarct volume was described by cresyl violet staining. The unstained region showed the infarct area. *$p < 0.05$ versus MCAO + miR-466c control. D. BBB permeability was examined by Evans blue leakage assay. *$p < 0.05$ versus sham group, #$p < 0.05$ versus MCAO + miR-466c control.

tigated. MiR-466c mimics or miR-466c control was injected into cerebral ischemia rats after MCAO through the stereotactic apparatus. Observations showed no symptoms of neurological impairment in the sham group and remarkably severe neurological deficit in MCAO surgery (**Figure 2**). Concordantly, compared with miR-466c control group, introduction of miR-466c caused a significant increase of neurological score after MCAO (**Figure 2A**). Moreover, elevated brain water content was enabled in a manner associated with miR-466c above control group following MCAO (**Figure 2B**). Meanwhile, cresyl violet stain assay described a broader unstained area in brain tissue in the presence of miR-466c (**Figure 2C**), suggesting addition of miR-466c contributed to ischemic infarct. Similarly, miR-466c triggered more leakage of Evans blue dye after the onset of MCAO (**Figure 2D**). These results suggested that accumulation of miR-466c exacerbated brain injury on cerebral ischemia.

Introduction of miR-466c facilitates BMECs permeability after OGD

To further explore the interaction of miR-466c with BBB permeability, an OGD model was established in BMECs. As expected, expression of miR-466c was drastically inhibited at 2 hours after OFD and later faintly regained (**Figure 3A**). However, expression of IGF-1 exhibited an opposite trend in BMECs after OGD at mRNA and protein levels, respectively (**Figure 3B** and **3C**). Furthermore, transfections were performed into BMECs after OGD with miR-466c mimics or control. Transfection efficiencies were validated by elevated levels of miR-466c compared with their counterparts (**Figure 3D**). Indeed, OGD induced the flux of FITC-dextran and a strong increase of permeability with introduction of miR-466c in BMECs (**Figure 3E**). Taken together, these data demonstrate that introduction of miR-466c enhances BMEC permeability after OGD.

IGF-1 is bind directly to miR-466c

Next, it was considered to probe the interaction between miR-466c and IGF-1. Bioinformatics analysis hypothesized a binding site between miR-466c and 3'-UTR of IGF-1, predicted by online tool TargetScan, suggesting that IGF-1 might be a direct target gene of miR-466c (**Figure 4A**). Therefore, luciferase assays showed a remarkable reduction of luciferase activity with the presence of miR-466c mimics in BMECs transfected with IGF-1 3'-UTR WT compared to control, but little effect was observed

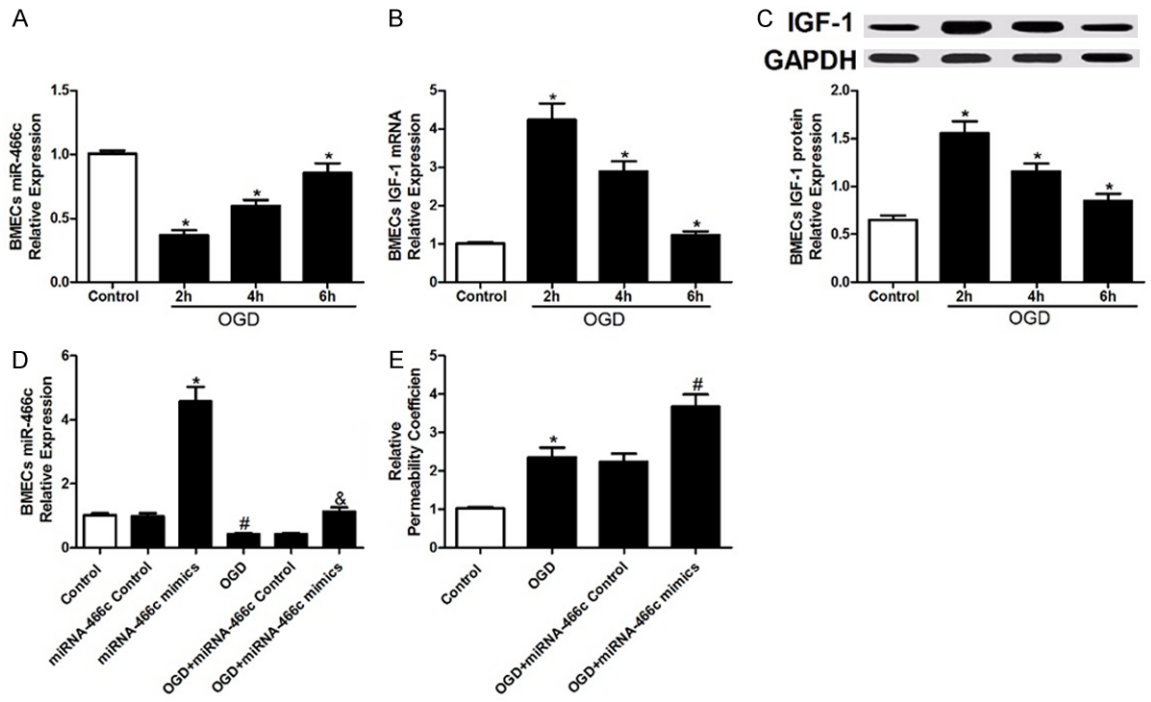

Figure 3. Addition of miR-466c increases BMECs permeability after OGD. A. The abundance of miR-466c was detected by qRT-PCR in BMECS at 2, 4, and 6 hours after OGD. *$p < 0.05$ versus control. B and C. IGF-1 expression in OGD-treated BMECs was examined at mRNA and protein levels, respectively. D. The abundance of miR-466c was analyzed in BMECs with miR-466c mimics or control transfection. *$p < 0.05$ versus miR-466c control, #$p < 0.05$ versus control, &$p < 0.05$ versus OGD + miR-466c control. E. Permeability coefficient was evaluated by the flux of FITC-dextran. *$p < 0.05$ versus control, #$p < 0.05$ versus OGD + miR-466c control.

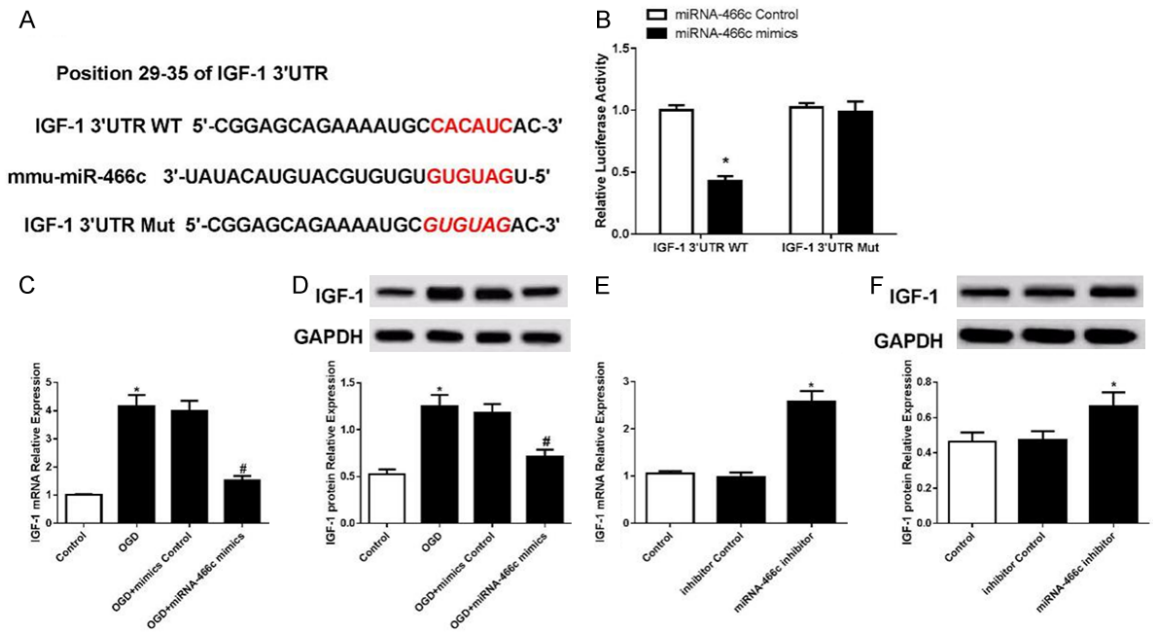

Figure 4. IGF-1 is a target of miR-466c. (A) Wild-type (IGF-1 3'-UTR WT) and mutant (IGF-1 3'-UTR Mut) of putative miR-466c targeting sequences. (B) Analysis of luciferase activity was performed in BMECs transfected by miR-466c mimics and IGF-1 3'-UTR WT or Mut compared with negative control. *$p < 0.05$ versus miR-466c control. (C and D) The abundance of IGF-1 was analyzed at the RNA and protein levels in BMECs after OGD in the presence or (E and F) absence of miR-466c. *$p < 0.05$ versus control, #$p < 0.05$ versus OGD + miR-466c mimics control.

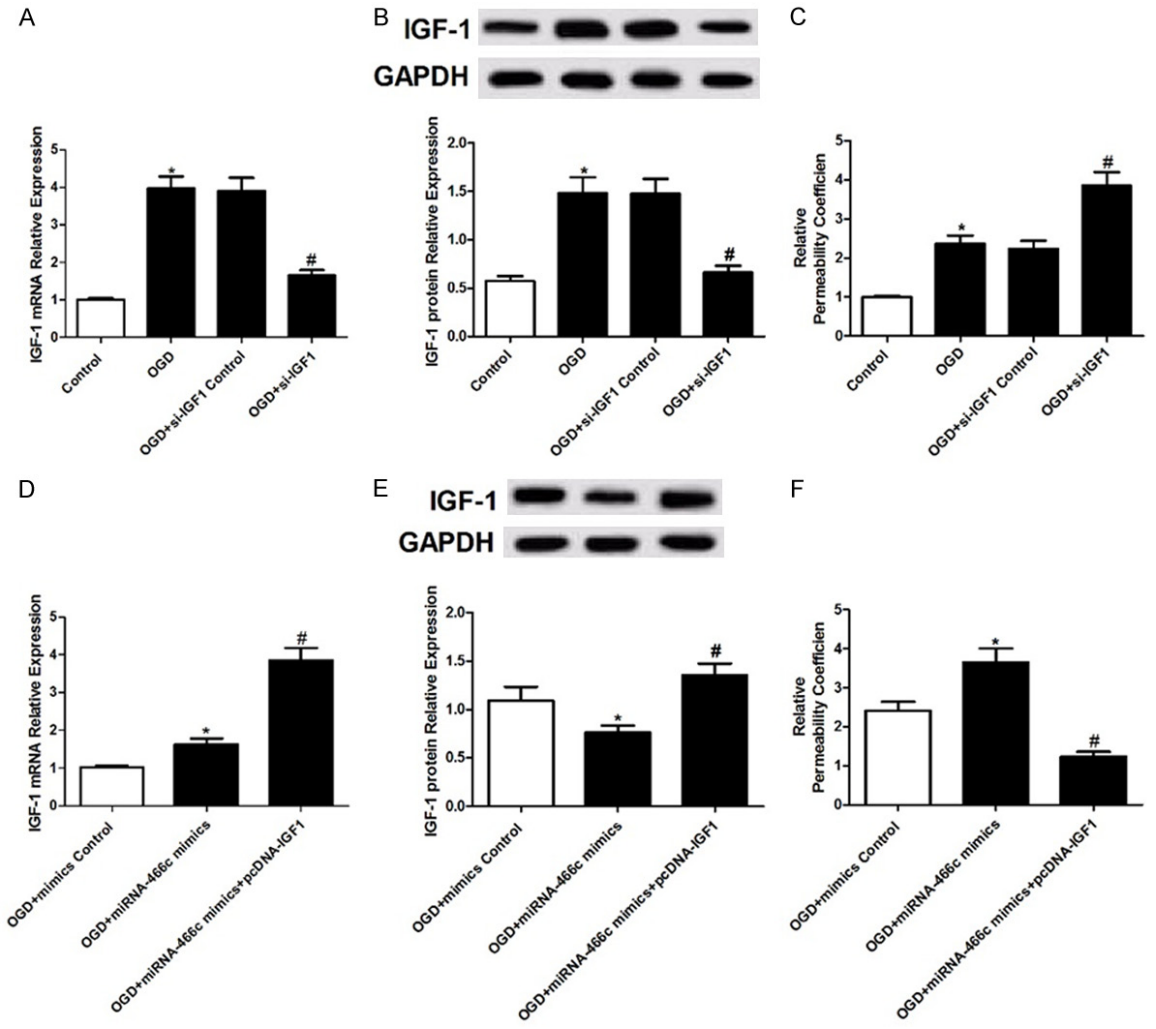

Figure 5. IGF-1 attenuates the effect of miR-466c on BMECs permeability. (A and B) The abundances of IGF-1 were analyzed at mRNA and protein levels in BMECs after OGD in the absence of IGF-1. *$p < 0.05$ versus control, #$p < 0.05$ versus OGD + si-IGF-1 control. (C) IGF-1 depletion increased the BMECs permeability after OGD. *$p < 0.05$ versus control, #$p < 0.05$ versus OGD + si-IGF-1 control. (D and E) Addition of IGF-1 reversed regulation of miR-466c on production of IGF-1 mRNA and protein in BMECs after OGD. *$p < 0.05$ versus OGD + miR-466c mimics control, #$p < 0.05$ versus OGD + miR-466c mimics. (F) Introduction of IGF-1 attenuated the function of miR-466c on BMECs permeability after OGD. *$p < 0.05$ versus OGD + miR-466c mimics control, #$p < 0.05$ versus OGD + miR-466c mimics.

in those transfected with IGF-1 3'-UTR Mut (**Figure 4B**). Further, the abundance of IGF-1 was decreased by addition of miR-466c in BMECs after OGD at mRNA and protein levels, respectively (**Figure 4C** and **4D**). In contrast, abrogation of miR-466c by miR-466c inhibitor resulted in increased abundance of IGF-1 mRNA and protein compared to inhibitor control (**Figure 4E** and **4F**). These results show that IGF-1 might be a candidate target of miR-466c and enrichment of miR-466c lowers expression of IGF-1.

Presence of IGF-1 counteracts BMECs permeability following addition of miR-466c

To investigate if miR-466c modulated the poor outcome of BMECs permeability through IGF-1, si-IGF-1 or pcDNA-IGF-1 was introduced into BMECs. As a result, interference of IGF-1 blocked IGF-1 expression at mRNA and protein levels in BMECs after OGD (**Figure 5A** and **5B**). Moreover, depletion of IGF-1 induced the accumulation of FITC-dextran on para-cellular in BMECs after OGD (**Figure 5C**). In contrast, introduction of pcDNA-IGF-1 promoted the abun-

dant production of IGF-1 mRNA and protein in BMECs with the presence of miR-466c after OGD (**Figure 5D** and **5E**). In addition, the positive effect of miR-466c on BMECs permeability was ablated following accumulation of pcDNA-IGF-1 compared between OGD + miR-466c mimics + pcDNA-IGF-1 and OGD + miR-466c mimics group (**Figure 5F**). All findings suggested that miR-466c regulated BMECs permeability after OGD through targeting IGF-1.

Discussion

In the current study, most attention was paid to the interaction of miR-466c with BBB permeability under cerebral ischemia both *in vivo* and *in vitro*. miR-466c was assessed as a promising therapeutic avenue for BBB protection upon cerebral ischemia. Recent works have suggested that miR-466 expression is impaired and might participate in cell proliferation and migration in colorectal cancer and prostate cancer [19, 20]. Likewise, the abundance of miR-466 was reduced during the tissue-engineered vascular graft or liver regeneration in rat models [21, 22]. Similarly, our data show a great loss of miR-466c abundance *in vivo* rats MCAO and *in vitro* BMECs OGD models, suggesting that miR-466c might play a pivotal role in cerebral ischemia.

BBB disruption has been shown to take part in cerebral ischemia [23], and miRNAs were reported to have an impact on the outcome of BBB dysfunction [24]. Cerebral deficit detection has been typically performed with the analyses of neurological score, brain water content, infarct volume, as well as BBB permeability. Introduction of miR-132 lessened BBB permeability and brain water content in mice on intracerebral hemorrhage [25]. Furthermore, addition of miR-216a might also induce reduction of neurological score, brain water content, and infarct volume in mice after MCAO [26]. However, our results describe accumulation of miR-466c which deteriorated the cerebral deficit and revealed elevated neurological score, brain water content, infarct volume, and BBB permeability. This is also consistent with the finding of miR-18a that was impaired and addition of it worsened brain injury in ischemic stroke [27]. This study also showed that cerebral ischemia induced IGF-1 expression. Generally, IGF-1 was considered as a novel approach to control the development and clinical features in patients with ischemia stroke [28]. Such work proposed IGF-1 could decrease infarct volume and improve neurologic function upon cerebral ischemia [29]. Furthermore, former efforts have suggested that IGF-1 is required for BBB permeability in rat models or in the clinic [30, 31].

Since functional miRNAs contributed to brain insult by regulating mRNA expression on ischemic stroke [9], it was further hypothesized that a link must exist between miR-466c and IGF-1. The former finding suggested miR-466 could repress lymph-angiogenesis via targeting prospero homeobox 1 during alkali burn corneal injury [32]. Moreover, miR-466 might be involved in modulating inositol requiring enzyme 1 and diabetic wound healing [33]. As expected, TargetScan online described the binding sites between miR-466c and 3'-UTR of IGF-1. Using another approach to analyze the prediction of IGF-1 as a target of miR-466c, validated by luciferase assay, it was proposed that addition of miR-466c lowered the abundance of IGF-1. On the basis of previous demonstrations, miR-466c was tested to determine whether it could ameliorate BBB permeability by targeting IGF-1 after cerebral ischemia.

The available evidence indicated in patients with cerebral ischemia, miR-223 was associated with ischemia stroke through modulating the abundance of IGF-1 [34]. Similarly, other miRNAs, such as miRNA Let7f and miR-29a, mediated IGF-1-like neuroprotection or reperfusion injury following ischemia stroke [35, 36]. Here, a protocol was developed with introduction of si-IGF-1 or pcDNA-IGF-1 and addition of IGF-1 was found to attenuate BBB permeability. This was afforded by the presence of abundant miR-466c upon cerebral ischemia. As described by previous study, IGF-1 was targeted by miR-29 and might serve important function in brain ischemia [37]. Elevated IGF-1 level by miR-320 abrogation might protect against ischemia and reperfusion injury in Wistar rats [38]. Seeing that the mechanisms of cerebral ischemia and BBB are complex, signaling pathways regulated by miR-466c need more attention for the treatment of ischemia injury in future.

Conclusion

In conclusion, this effort provided insight into the link between miR-466c and BBB permeability upon cerebral ischemia. Here cerebral

ischemia hindered the expression of miR-466c and enhanced expression of IGF-1. Addition of miR-466c stimulated BBB permeability on cerebral ischemia by targeting IGF-1, indicating that miR-466c might present a potential therapeutic targeting opportunity of cerebral ischemia.

Disclosure of conflict of interest

None.

Address correspondence to: Zhijun Ye, Department of Neurosurgery, Jinhua Central Hospital, No.351, Mingyue Street, Wucheng District, Jinhua City, 321001, Zhejiang Province, China. Tel: +86-0579-8233-8512; E-mail: 154dkjfgdu441@sina.com

References

[1] Turner RJ and Sharp FR. Implications of mmp9 for blood brain barrier disruption and hemorrhagic transformation following ischemic stroke. Front Cell Neurosci 2016; 10: 56.

[2] Sifat A, Vaidya B and Abbruscato T. Blood-brain barrier protection as a therapeutic strategy for acute ischemic stroke. AAPS J 2017; 19: 957-972.

[3] Bartel D. MicroRNAs: genomics, biogenesis, mechanism, and function. Cell 2004; 116: 281-297.

[4] Pan Y, Sun Z and Feng D. The role of microrna in traumatic brain injury. Neuroscience 2017; 367: 189-199.

[5] Ma Q, Dasgupta C, Li Y, Huang L and Zhang L. MicroRNA-210 suppresses junction proteins and disrupts blood-brain barrier integrity in neonatal rat hypoxic-ischemic brain injury. Int J Mol Sci 2017; 18.

[6] Wang X, Suofu Y, Akpinar B, Baranov S, Kim J, Carlisle D, Zhang Y and Friedlander R. Systemic antimiR-337-3p delivery inhibits cerebral ischemia-mediated injury. Neurobiol Dis 2017; 105: 156-163.

[7] Sun P, Liu D, Jickling G, Sharp F and Yin K. MicroRNA-based therapeutics in central nervous system injuries. J Cereb Blood Flow Metab 2018; 38: 1125-1148.

[8] Shyamasundar S, Jadhav S, Bay B, Tay S, Kumar S, Rangasamy D and Dheen S. Analysis of epigenetic factors in mouse embryonic neural stem cells exposed to hyperglycemia. PLoS ONE 2013; 8: e65945.

[9] Jimenez-Mateos E. Role of MicroRNAs in innate neuroprotection mechanisms due to preconditioning of the brain. Front Neurosci 2015; 9: 118.

[10] Toth P, Tucsek Z, Tarantini S, Sosnowska D, Gautam T, Mitschelen M, Koller A, Sonntag W, Csiszar A and Ungvari Z. IGF-1 deficiency impairs cerebral myogenic autoregulation in hypertensive mice. J Cereb Blood Flow Metab 2014; 34: 1887-1897.

[11] Okoreeh A, Bake S and Sohrabji F. Astrocyte-specific insulin-like growth factor-1 gene transfer in aging female rats improves stroke outcomes. Glia 2017; 65: 1043-1058.

[12] Cui X, Chopp M, Zacharek A, Karasinska J, Cui Y, Ning R, Zhang Y, Wang Y and Chen J. Deficiency of brain ATP-binding cassette transporter A-1 exacerbates blood-brain barrier and white matter damage after stroke. Stroke 2015; 46: 827-834.

[13] Park MJ and Sohrabji F. The histone deacetylase inhibitor, sodium butyrate, exhibits neuroprotective effects for ischemic stroke in middle-aged female rats. J Neuroinflammation 2016; 13: 300.

[14] Lekic T, Flores J, Klebe D, Doycheva D, Rolland W, Tang J and Zhang J. Intranasal IGF-1 reduced rat pup germinal matrix hemorrhage. Acta Neurochir Suppl 2016; 121: 209-212.

[15] Zemva J and Schubert M. The role of neuronal insulin/insulin-like growth factor-1 signaling for the pathogenesis of alzheimer's disease: possible therapeutic implications. CNS Neurol Disord Drug Targets 2014; 13: 322-337.

[16] Bake S, Selvamani A, Cherry J and Sohrabji F. Blood brain barrier and neuroinflammation are critical targets of IGF-1-mediated neuroprotection in stroke for middle-aged female rats. PLoS ONE 2014; 9: e91427.

[17] Wang L, Zhao H, Zhai Z and Qu L. Protective effect and mechanism of ginsenoside Rg1 in cerebral ischaemia-reperfusion injury in mice. Biomed Pharmacother 2018; 99: 876-882.

[18] Wang J, Tang Y, Zhang W, Zhao H, Wang R, Yan Y, Xu L and Li P. Insulin-like growth factor-1 secreted by brain microvascular endothelial cells attenuates neuron injury upon ischemia. FEBS J 2013; 280: 3658-3668.

[19] Tong F, Ying Y, Pan H, Zhao W, Li H and Zhan X. MicroRNA-466 (miR-466) functions as a tumor suppressor and prognostic factor in colorectal cancer (CRC). Bosn J Basic Med Sci 2018; 18: 252-259.

[20] Colden M, Dar A, Saini S, Dahiya P, Shahryari V, Yamamura S, Tanaka Y, Stein G, Dahiya R and Majid S. MicroRNA-466 inhibits tumor growth and bone metastasis in prostate cancer by direct regulation of osteogenic transcription factor RUNX2. Cell Death Dis 2017; 8: e2572.

[21] Hibino N, Best C, Engle A, Ghimbovschi S, Knoblach S, Nath D, Ishibashi N and Jonas R. Novel association of mir-451 with the inci-

dence of tevg stenosis in a murine model. Tissue Eng Part A 2016; 22: 75-82.
[22] Werner W, Sallmon H, Leder A, Lippert S, Reutzel-Selke A, Morgül M, Jonas S, Dame C, Neuhaus P, Iacomini J, Tullius S, Sauer I and Raschzok N. Independent effects of sham laparotomy and anesthesia on hepatic microRNA expression in rats. BMC Res Notes 2014; 7: 702.
[23] Yenari M and Han H. Neuroprotective mechanisms of hypothermia in brain ischaemia. Nat Rev Neurosci 2012; 13: 267-278.
[24] Toyama K, Spin J and Tsao P. Role of microRNAs on Blood brain barrier dysfunction in vascular cognitive impairment. Curr Drug Deliv 2017; 14: 744-757.
[25] Zhang Y, Han B, He Y, Li D, Ma X, Liu Q and Hao J. MicroRNA-132 attenuates neurobehavioral and neuropathological changes associated with intracerebral hemorrhage in mice. Neurochem Int 2017; 107: 182-190.
[26] Tian Y, Zhong D, Liu Q, Zhao X, Sun H, Jin J, Wang H and Li G. Upregulation of miR-216a exerts neuroprotective effects against ischemic injury through negatively regulating JAK2/STAT3-involved apoptosis and inflammatory pathways. J Neurosurg 2018; 1-12.
[27] Zhang L, Luo X, Chen F, Yuan W, Xiao X, Zhang X, Dong Y, Zhang Y and Liu Y. LncRNA SNHG1 regulates cerebrovascular pathologies as a competing endogenous RNA through HIF-1α/VEGF signaling in ischemic stroke. J Cell Biochem 2018; 119: 5460-5472.
[28] Kim H, Kim S, Park H, Chung J, Chun J, Yun D and Kim Y. Polymorphisms of IGFI contribute to the development of ischemic stroke. Exp Ther Med 2012; 3: 93-98.
[29] Liu X, Fawcett J, Thorne R, DeFor T and Frey W. Intranasal administration of insulin-like growth factor-I bypasses the blood-brain barrier and protects against focal cerebral ischemic damage. J Neurol Sci 2001; 187: 91-97.
[30] Benarroch E. Insulin-like growth factors in the brain and their potential clinical implications. Neurology 2012; 79: 2148-2153.
[31] Pang Y, Zheng B, Campbell L, Fan L, Cai Z and Rhodes P. IGF-1 can either protect against or increase LPS-induced damage in the developing rat brain. Pediatr Res 2010; 67: 579-584.
[32] Seo M, Choi J, Rho C, Joo C and Lee S. MicroRNA miR-466 inhibits Lymphangiogenesis by targeting prospero-related homeobox 1 in the alkali burn corneal injury model. J Biomed Sci 2015; 22: 3.
[33] Wang J, Qiu Y, Yang Z, Li L and Zhang K. Inositol-requiring enzyme 1 facilitates diabetic wound healing through modulating micrornas. Diabetes 2017; 66: 177-192.
[34] Wang Y, Zhang Y, Huang J, Chen X, Gu X, Wang Y, Zeng L and Yang G. Increase of circulating miR-223 and insulin-like growth factor-1 is associated with the pathogenesis of acute ischemic stroke in patients. BMC Neurol 2014; 14: 77.
[35] Selvamani A, Sathyan P, Miranda R and Sohrabji F. An antagomir to microRNA Let7f promotes neuroprotection in an ischemic stroke model. PLoS One 2012; 7: e32662.
[36] Wang L, Niu X, Hu J, Xing H, Sun M, Wang J, Jian Q and Yang H. After myocardial ischemia-reperfusion, mir-29a, and let7 could affect apoptosis through regulating igf-1. Biomed Res Int 2015; 2015: 245412.
[37] He J, Gao Y, Wu G, Lei X, Zhang Y, Pan W and Yu H. Bioinformatics analysis of microarray data to reveal the pathogenesis of brain ischemia. Mol Med Rep 2018; 18: 333-341.
[38] Song C, Liu B, Diao H, Shi Y, Zhang J, Li Y, Liu N, Yu Y, Wang G, Wang J and Li Q. Down-regulation of microRNA-320 suppresses cardiomyocyte apoptosis and protects against myocardial ischemia and reperfusion injury by targeting IGF-1. Oncotarget 2016; 7: 39740-39757.